Molecular Crystals and Liquid Crystals
Publication details, including instructions for authors and subscription information:
http://www.tandfonline.com/loi/gmcl20

Nematicons in Azobenzene Liquid Crystals

Svetlana V. Serak [a], Nelson V. Tabiryan [a] & Gaetano Assanto [b]
[a] BEAM Engineering for Advanced Measurements Co., 809 S. Orlando Ave., Suite I, Winter Park, FL, 32789, USA
[b] NooEL-Nonlinear Optics and OptoElectronics Lab., Via della Vasca Navale 84, 00146, Rome, Italy
Version of record first published: 11 May 2012.

To cite this article: Svetlana V. Serak , Nelson V. Tabiryan & Gaetano Assanto (2012): Nematicons in Azobenzene Liquid Crystals, Molecular Crystals and Liquid Crystals, 559:1, 202-213

To link to this article: http://dx.doi.org/10.1080/15421406.2012.658710

Mol. Cryst. Liq. Cryst., Vol. 559: pp. 202–213, 2012

ISSN: 1542-1406 print/1563-5287 online
DOI: 10.1080/15421406.2012.658710

Taylor & Francis
Taylor & Francis Group

Nematicons in Azobenzene Liquid Crystals

SVETLANA V. SERAK,[1,*] NELSON V. TABIRYAN,[1]
AND GAETANO ASSANTO[2]

[1]BEAM Engineering for Advanced Measurements Co., 809 S. Orlando Ave., Suite I, Winter Park, FL 32789 USA
[2]NooEL-Nonlinear Optics and OptoElectronics Lab., Via della Vasca Navale 84, 00146 Rome, Italy

We review our comprehensive investigation of light self-localization phenomena in planarly configured azobenzene liquid crystals. Cis-trans *isomerization of azobenzene molecules and related changes in the order parameter of the liquid crystals support a high nonlinear response and the formation of optical spatial solitons at microwatt excitations. We describe bright soliton angular steering, deflection, interleaving and merging, as well as dark solitons.*

Keywords *Cis-trans* isomerization; laser; liquid crystals; solitons

1. Introduction

The propagation of optical spatial solitons in nonlinear media and their perspective use for signal steering, readdressing, all-optical switching and other photonic applications have attracted growing interest in the past few years [1–4]. Liquid crystals (LCs) are excellent optical materials for these investigations, owing to extended spectral transparency, high electro-optic response and large nonlinearity [5–7]. In the nematic LC phase, the reorientation of the (elongated) organic molecules in the presence of an electromagnetic field is the basic mechanism for self-focusing, the latter enabling the generation of robust spatial optical solitons at low power levels [8–11] down to microwatts [12,13]. In addition, the nonlocality inherent to the dielectric response of a liquid mediates soliton stability in two transverse dimensions [14–17] as well as a variety of soliton-soliton [18–22], soliton-beam [23–25] and soliton-perturbation interactions [26–29].

While most soliton demonstrations were reported in nematic LC, the recent development and commercial availability of room temperature azobenzene nematic LC (azo-LC) [12,30] have stimulated the investigation of a nonlinear refraction mechanism related to photoinduced isomerization: rod-shaped azo molecules in the *trans*-form are bent into the *cis*-form when absorbing light in the ultraviolet (UV)-green region, the reverse process taking place with radiation at longer wavelengths. The accumulation of *cis*-isomers lowers the LC order parameter and can change the LC mesophase into the isotropic one. In azo-LCs containing a mixture of both *trans* and *cis* isomers, red light can increase the refractive

*Address correspondence to Svetlana V. Serak, BEAM Engineering for Advanced Measurements Co., 809 S. Orlando Ave., Suite I, Winter Park, FL 32789, USA. Phone: (407) 629-1282; Fax: (407) 629-0460. E-mail: svetlana@beamco.com

index for extraordinary waves and produce optical self-focusing owing to *cis-trans* photoisomerization of the azobenzene [12,31]. The resulting dielectric constant ε of the mixture can be expressed as:

$$\varepsilon = \varepsilon_{trans} N_{trans} + \varepsilon_{cis} N_{cis} \tag{1}$$

with N_{cis} and N_{trans} the fractions of *cis* and *trans* isomers, respectively, the weights being the corresponding dielectric constants at optical frequency [32]. Since both the dielectric properties and the order parameter of the azo-LC depend on the concentration of *trans* and *cis* isomers, photoisomerization modifies the refractive index of the mixture and mediates a novel type of optical nonlinearity which is efficient and relatively fast as compared to reorientational and thermal responses of nematic liquid crystals [33,34].

In this paper we show that the photoisomerization-induced nonlinear response of azo-LC can support self-focusing and the formation of optical spatial solitons or *nematicons* at wavelengths in the red even at μW power levels, offering a wealth of opportunities for their efficient steering and all-optical control with extra beams of various wavelengths. Furthermore, exploiting the photoinduced reduction of the order parameter, the resulting self-defocusing response allows generating optical dark spatial solitons.

2. Experiments and Discussion

2.1 Bright Solitons in Nematic Azo-LC

We carried out our experiments using a standard setup as sketched in Fig. 1(a), with a continuous wave Helium-Neon laser oscillating at $\lambda = 632.8$ nm. The beam was linearly polarized – in either an extraordinary (e−) or ordinary (o−) wave with the aid of a twisted LC cell, and then focused into a planar glass cell with either a 20 X microscope objective or a 35 mm lens. Light propagation in the sample was monitored with an inverted microscope and a high-resolution Silicon CCD camera. The azo-LC layer in between the glass walls was 80-μm thick and planar oriented with molecular director **n** parallel to the x-axis, i.e.

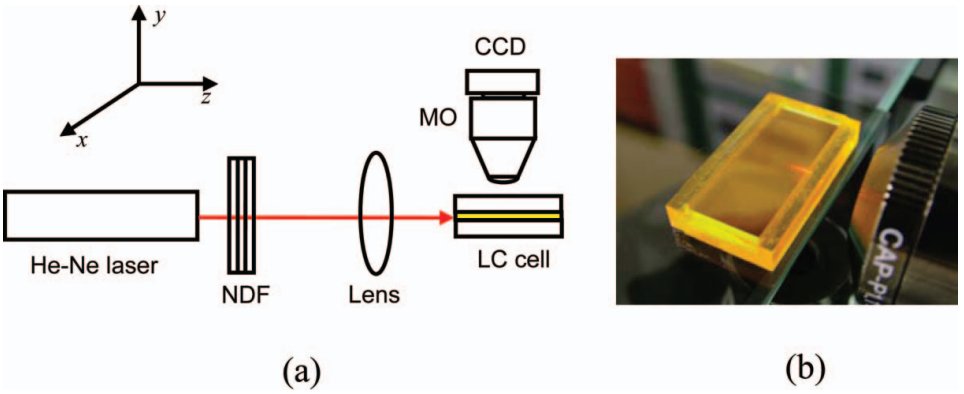

Figure 1. (a) Setup for generation and observation of spatial solitons and (b) photo of a planar azo-LC sample. The LC sample was 23 mm wide, 10 mm long and 0.08 mm thick. NDF stands for neutral density filters.

orthogonal to the wavevector of the incident beam (s). Fig. 1(b) displays a photograph of the sample.

In our measurements we employed a variety of azo-LC materials (available from beamco.com). For the study in the visible spectrum presented hereby we used either the azobenzene LC no. 1005 or azo-LC no. 1205, with clearing temperatures of 49 and 59°C, respectively. At 22°C and for light at 632.8 nm the refractive indices of birefringent azo-LC 1005 (1205) in the *trans* state are $n_{||} = 1.726$ ($n_{||} = 1.751$) and $n_{\perp} = 1.540$ ($n_{\perp} = 1.541$) and the value in the saturated *cis* state is $n_{cis} = 1.631$ [35]. These two azo-LC materials exhibit similar linear and nonlinear properties in the visible; hence, all the results presented hereby can be considered characteristic of the entire class of azo-LC with a positive birefringence $n_{||} - n_{\perp} > 0$. For extraordinarily-polarized incident light with electric field parallel to the LC director **n** it is $\varepsilon_{\text{cis}} - \varepsilon_{\text{trans}} = \varepsilon_{\text{cis}} - \varepsilon_{||} < 0$; hence, *cis-trans* light-induced isomerization increases the *e*-refractive index, Fig. 2(a). Therefore, an intense enough *e*-polarized red laser beam can reduce the concentration of *cis* isomers and cause self-focusing and the formation of a spatial soliton, as sketched in Fig. 2(b). Conversely, if the incident beam is polarized orthogonal to the LC director (ordinary polarization), then $\varepsilon_{cis} - \varepsilon_{trans} = \varepsilon_{cis} - \varepsilon_{\perp} > 0$ and light undergoes diffraction, as illustrated in Fig. 2(c).

Spatial solitons were readily generated at power levels even below milliWatt, as shown in Fig. 3(a): the diffraction of the *extraordinary*-wave beam starts to decrease at microwatts powers, giving rise to stable solitons from around 25 μW up to 3.5 mW. Above the latter value the beam divergence increases again, probably due to the interplay between saturation

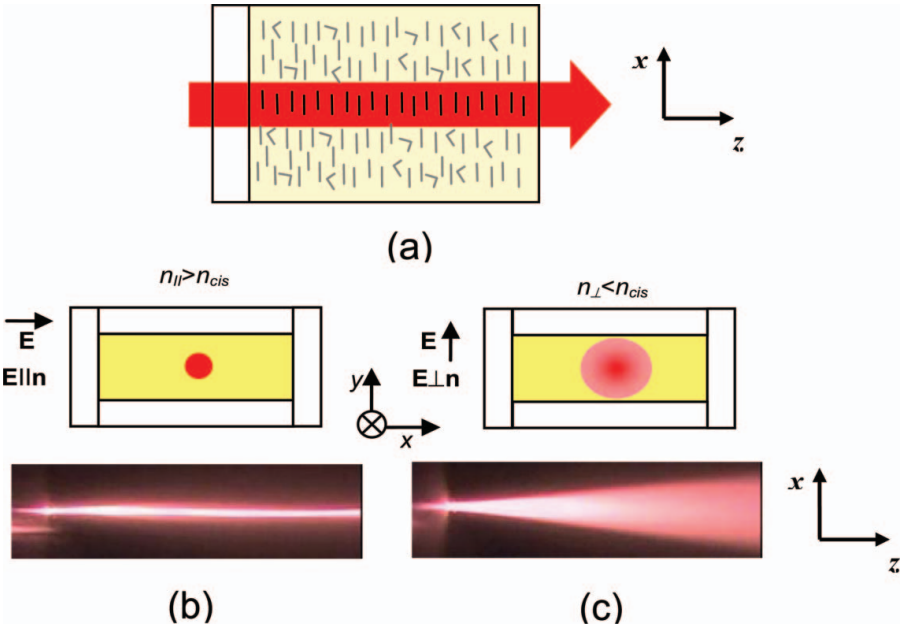

Figure 2. Light beam propagating in the azo-LC planar sample. (a) The beam transforms *cis* isomers into *trans* isomers, aligned along the rubbing direction *x*. (b) An intense extraordinary beam with **E**|| **n** gets self-focused and can form a soliton, as shown in the photograph for He-Ne excitation. The transverse size of the soliton is 22 μm. (c) An ordinary polarized beam diffracts (photograph). In both experiments ((b) and (c)) the red laser beam is launched from the left at a power of 43 μW and propagated for about 1 mm.

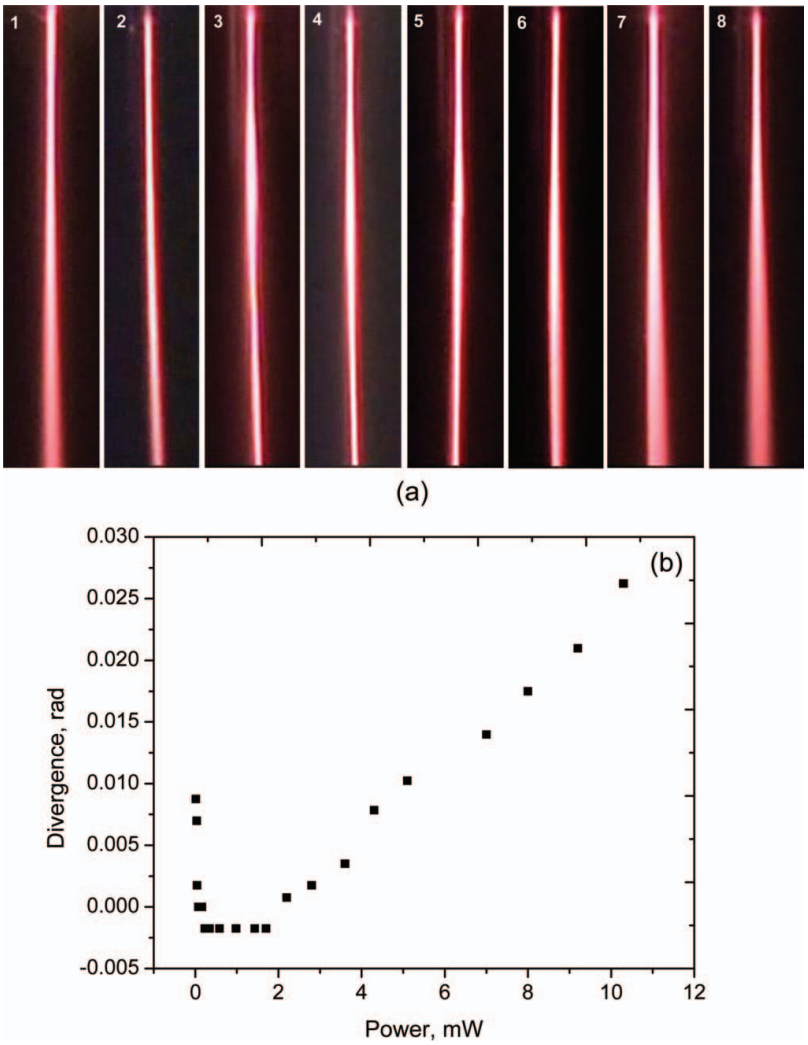

Figure 3. (a) *xz* evolution of an extraordinary beam for various excitations: 1–10 μW; 2–33 μW, 3–72 μW, 4–340 μW; 5–0.98 mW; 6–2.8 mW; 7–5.2 mW; 8–8 mW. Here the medium is azo-LC 1005, and the (shown) propagation length is 0.8 mm. (b) Divergence of the He-Ne beam versus power measured at 0.69 mm from the input.

in the reorientational response and the insurgence of thermal effects. Fig. 3(b) plots the measured divergence (i.e. size) versus excitation. The time dynamics of soliton formation is faster at higher excitations, well below 100 ms for sub-mW powers, as visible in Fig. 4.

Despite the nature of the nonlinearity in azo-LC, nonlocality plays an important role in photoisomerization, as in reorientational and thermal responses [15,16,36]. Owing to the interplay of nonlocality and reorientational effects at higher powers, breathing [16] (Fig. 5) and instabilities could be observed as well, with the formation of multiple solitons from a single input beam, as in Fig. 5. At variance with a previous report in nematic LC [37],

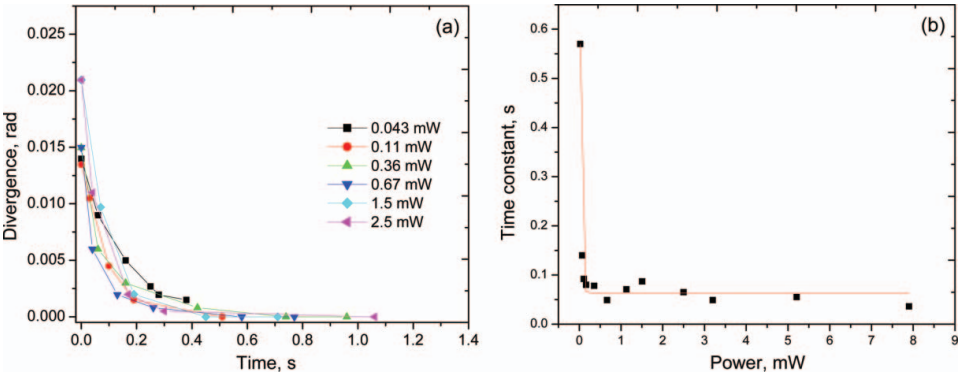

Figure 4. (a) Temporal dynamics of self-focusing (decreasing divergence) of an extraordinary beam in azo-LC 1205 for various input powers. (b) Response time versus excitation.

no special beam focusing was required to yield the latter result, relying on transverse modulational instability in order to seed the effect in the relatively wide input beam.

Due to long lifetime of *cis* isomers in the sample, a (relatively) fast transverse displacement of the cell with respect to the input laser beam resulted in the lateral bending deflection of the soliton, progressively reducing in time as shown by the photo sequence of Fig. 6(a). Here the initial shift is of the order of the beam size. The redistribution of the isomers around the beam restored the straight propagation of the soliton with typical times of the order of a few seconds, as visible in Fig. 6(b) [12].

2.2 Bright Soliton Merging in Nematic Azo LC

LCs exhibit a highly nonlocal behavior associated to their fluid state and the elastic forces linking their molecules [5–7]. As stated above, a nonlocal response also characterizes azo-LC owing to diffusion of isomers generated by and along the laser beam. Therefore, even spatial solitons in azo-LC can sense the presence of extra solitons or beams nearby and can interact as elastic or inelastic particles [18–20]. Typically, the index gradient resulting from the nonlocal index perturbation gives rise to an attractive force bending the soliton trajectory(ies) and substantially insensitive to coherent effects associated to their relative phase. Figure 7 shows formation of two solitons and their interleaving in azo-LC for different launching conditions that could not be precisely controlled in the experiment. The power of the beam was 3.2 mW in both cases.

For two equi-power beams of 0.63 mW launched in an 80 μm-thick cell with azo-LC 1005, we investigated the dynamics of soliton attraction, interleaving and, eventually,

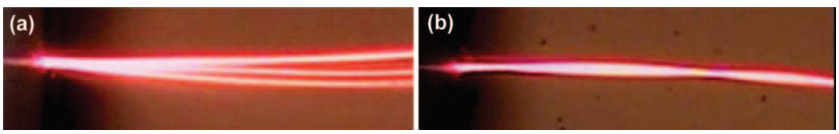

Figure 5. Examples of spatial solitons generated by a red beam of 3.2 mW power. The beams are injected in azo-LC 1205 from the left; the propagation length is 0.8 mm.

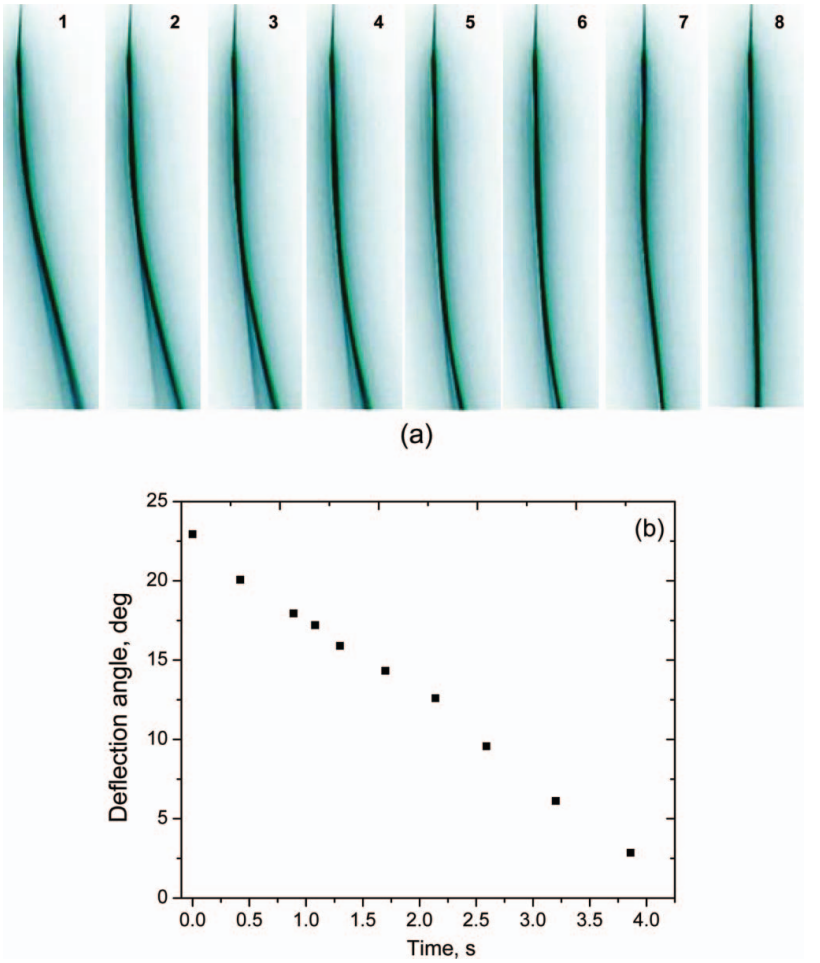

Figure 6. (a) Photographs (inverted images) of soliton deflection produced by a cell translation. Snapshots taken at: 1 − t = 0.4 s; 2 – t = 0.9 s; 3 – t = 1.08 s; 4 – t = 1.7 s, 5 – t = 1.7 s; 6 – t = 2.14 s; 7 – t = 2.6 s; 8 – t = 3.9 s. The propagation length is 0.8 mm. (b) Time dynamics of soliton "straightening" after deflection (Media 1). Here we employed the azo-LC 1205 and a 3.2 mW He-Ne beam.

merging. Typical results for two input beams injected at a relative angle of 4.3° are shown in Fig. 8. The merging process took a few seconds after mutual oscillations and interleaving, and was evaluated in time by measuring the separation between the self-localized beams at a given propagation distance in the material, as graphed in Fig. 9.

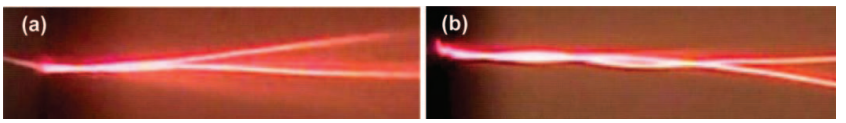

Figure 7. Examples of mutual interactions of spatial solitons in azo-LC with input beams launched from left to right and propagating for 0.8 mm.

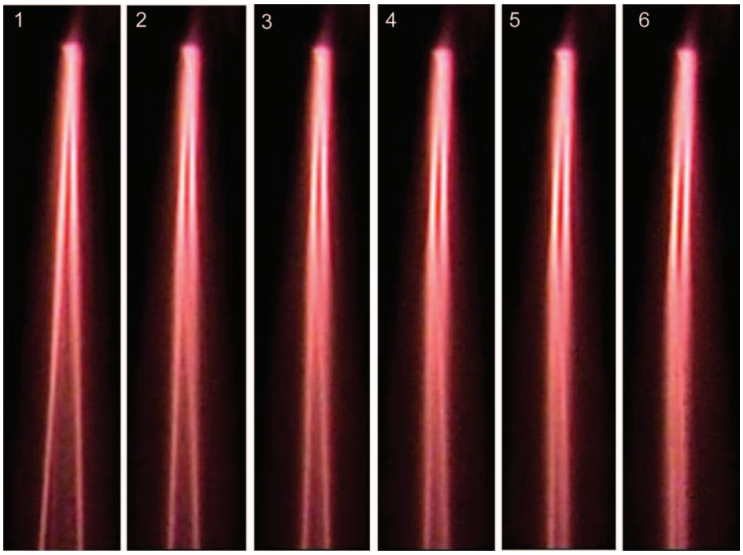

Figure 8. Temporal dynamics of merging solitons in azo-LC 1005 (Media 2). The time sequence is: 1 – 0 s; 2 – 1.12 s; 3 – 1.48 s; 4 – 2.08 s; 5 – 2.9 s; 6 – 3.58 s. The initial angle between the beams is 4.3° inside the medium. The visible area in the photographs is 0.8 mm × 0.16 mm. The beams carry equal powers of 0.63 mW at the input.

2.3. Bright Channels in the Photoinduced Isotropic State of Azo LC

It has been shown that the photoinduced isotropic (PI) state of azo LCs exhibits one of the highest known nonlinear optical refraction among isotropic materials [35]. The optical nonlinearity of these media is large in a wide band of the visible spectrum and it possesses high, over 90%, transmission for wavelengths in the red. The PI state of azo LCs is

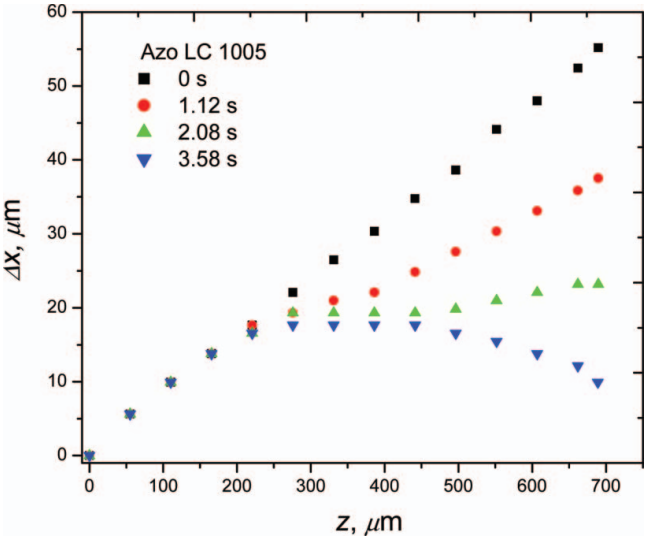

Figure 9. Separation between solitons in azo-LC 1005 versus propagation distance at various times following the excitation.

obtained by exposing it to UV-blue radiation; the accumulation of a critical concentration of the non-mesogenic *cis* form of the azo molecules drives the material into the isotropic phase. Noteworthy, the PI state of an azo LC is substantially different from the thermally induced isotropic (TI) phase. The TI state consists primarily of *trans* molecules whereas the PI state of azo LCs is a mixture of *trans* and *cis* isomers with a substantial concentration of *cis* molecules. Removal of the heat source results in fast (ms to seconds) relaxation of the TI phase back to the mesophase. The PI state of azo LCs can last tens of hours, since the dark relaxation is governed by the lifetime of *cis* isomers at a fixed temperature. Most importantly for optical applications, the absorption spectrum and the refractive index of the PI state differs from the TI state: $n_{TI} = 1.66$ and $n_{PI} = 1.63$ at wavelength $\lambda = 632.8$ nm [35].

The interaction of a He-Ne laser beam with the PI state of azo LCs revealed a few interesting peculiarities. The beam, initially nearly invisible due to low scattering losses in the isotropic phase, became visible first at the end of the cell, opposite to the input. This is attributed to an initially weak self-focusing, with higher power densities near the end of the propagation distance and, therefore, enhanced efficiency of the *cis-trans* isomerization towards the critical region of photoinduced isotropic-nematic phase transition. Thus, the enhanced fluctuations resulted in augmented light scattering making the beam visible [38]. The extent of the isomerized region increased in time revealing the self-induced channel, Fig. 10, which shifted closer and closer to the cell entrance. Such rather complex and not entirely explained space-time dynamics resulted in "fireworks" launched from the output to the input. Eventually, *cis-trans* isomerization made the beam visible by the cell input, Fig. 11.

2.4. Dark Solitons Via Light-Induced Reduction of the Order Parameter

Dark solitons are supported by a self-defocusing response and are intensity notches with a π phase jump in a uniform background. [1] Even these self-localized waves can act as self-induced waveguides .

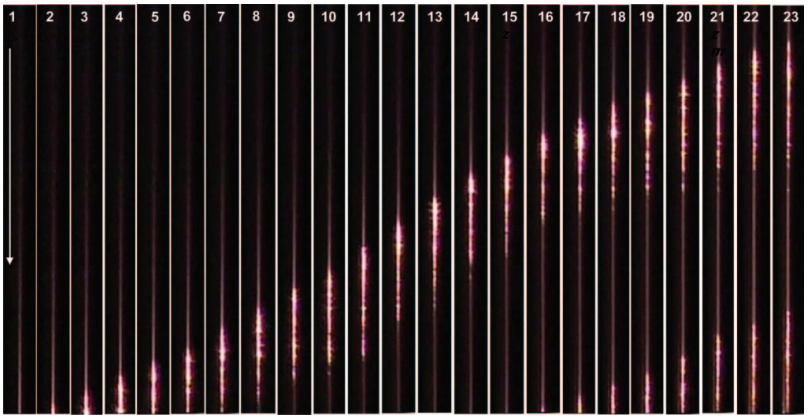

Figure 10. Light propagating away from the input interface. Snapshots at: 1 – t = s, 2 – t = 0.07 s; 3 – t = 0.1 s; 4 − t = 0.13 s, 5 − t = 0.16 s; 6 − t = 0.2 s; 7 − t = 0.26 s; 8 − t = 0.32 s; 9 − t = 0.39 s, 10 − t = 0.45 s, 11 − t = 0.55 s; 12 − t = 0.64 s, 13 − t = 0.77 s, 14 − t = 0.96 s, 15 − t = 1.09 s, 16 − t = 1.22 s; 17 − t = 1.35 s, 18 − t = 1.48 s; 19 − t = 1.6 s; 20 − t = 1.73 s; 21 − t = 1.89 s; 22 − t = 2.05 s; 23 − t = 2.18 s. The used azo LC 1205 was pre-exposed for 38 min using an UV lamp ($\lambda = 365$ nm, $I = 10$ mW/cm^2). The 5.2 mW red laser beam was focused at the input with a 35-mm focal length lens. The propagation distance is 0.8 mm. The white arrow indicates the direction of the launch beam.

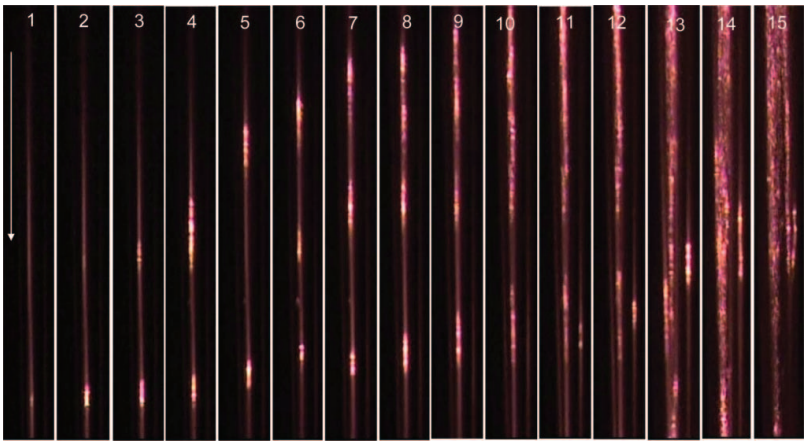

Figure 11. Dynamics of self-focused bright spots in isotropic azo-LC. Time is: 1 – t = 0 s; 2 – t = 0.09 s; 3 – t = 0.13 s; 4 – t = 0.32 s; 5 – t = 1.2 s; 6 – t = 1.8 s; 7 – t = 2.4 s; 8 – t = 2.8 s; 9 – t = 3.14 s; 10 – t = 3.84 s; 11 – t = 4.77 s; 12 – t = 5.65 s; 13 – t = 6.26 s; 14 – t = 8.75 s; 15 – t = 13.4 s (Media 3). The azo LC 1205 was pre-exposed for 30 minutes using a UV lamp ($\lambda = 365$ nm, $I = 10$ mW/cm^2). The 3.4 mW red laser beam was focused at the cell entrance with a 20X microscope objective. The propagation length was 0.8 mm. The arrow on the left indicates the incidence beam direction.

To obtain a self-defocusing nonlinearity, we used a mixture of the commercial nematic LC 5CB with the mesogenic azo dye CPND [39,40] (10% in weight), in a standard planar cell of thickness 9 μm and with inner interfaces treated to obtain homeotropic anchoring, i. e. with molecular director perpendicular to the confining surfaces.

By illuminating the sample with green light ($\lambda = 532$ nm) of wavelength within the absorption band we could lower the order parameter as the LCs rearranged around the excited-state dye molecules. First we focused a 2 μm waist beam and observed that the extraordinary wave (electric field along x) self-defocused, whereas the ordinary wave (field along y) self-focused (Fig. 12).

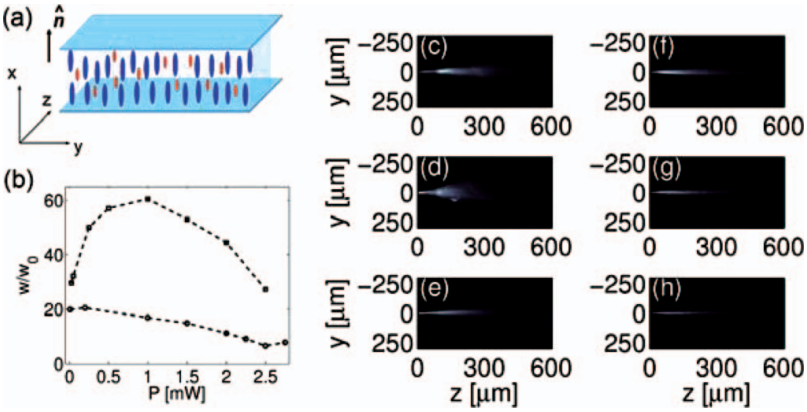

Figure 12. (a) Sketch of the sample. The blue ellipses represent the LC molecules, the red ones the azo dye. (b) Waist versus power of an input Gaussian beam, for ordinary (bottom line) and extraordinary (top line) polarizations. (c–h) Photographs of ordinary (c–e) and extraordinary (f–h) green beams launched at 0.1, 1 and 2 mW respectively.

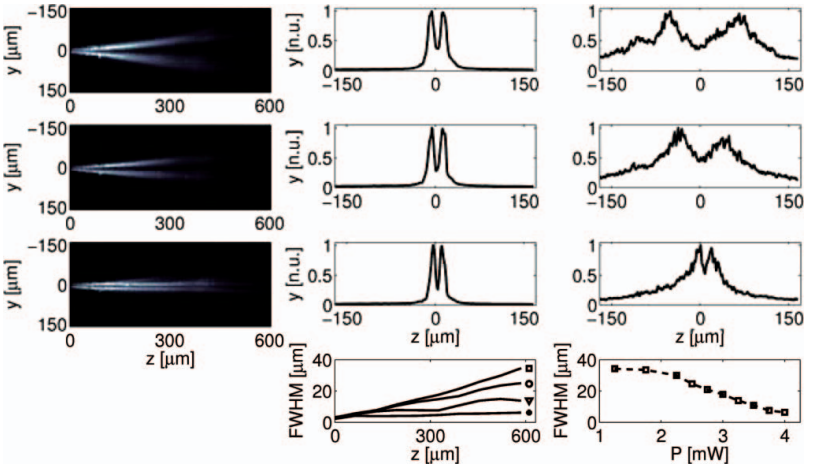

Figure 13. Dark spatial solitons in azo nematic LCs. Photographs (left), input (center row) and output (right) profiles for $P = 1$ (first row), 2 (second row) and 4 mW (third row), respectively. The bottom graphs display the FWHM of the notch versus propagation (left) for $P = 1$ (squares), 2 (circles), 3 (triangles) 4 mW (dots) and in $z = 0.5$ mm versus excitation (right).

Then we launched a bell-shaped beam with a one-dimensional notch on a wide bright background along *y*. By increasing the launch power of an extraordinarily polarized beam (Fig. 13), self-defocusing progressively narrowed the notch. At 4 mW we observed a nearly constant FWHM, consistent with the propagation of a dark soliton [41]. To validate the generation of a dark spatial soliton, we coupled a low power near-infrared probe ($\lambda =$ 1064 nm) (transmitted by the mixture) and studied its confinement in the dark soliton excited in the green. As shown in Fig. 14, when the weak probe was ordinarily polarized it sensed a refractive index dip (due to change in order parameter) and diffracted; when

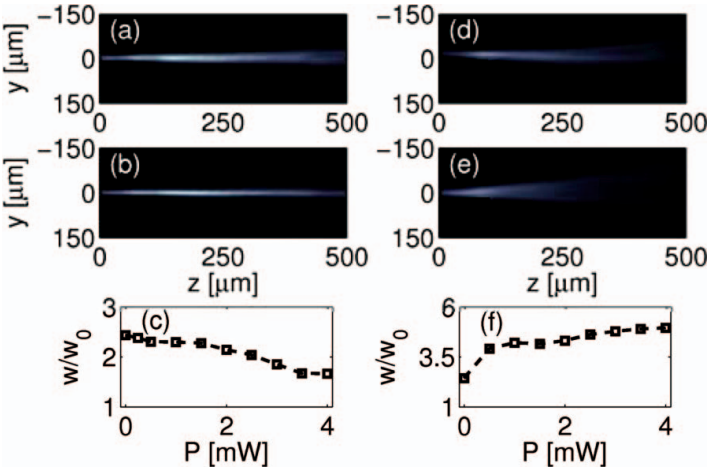

Figure 14. Collinear near-infrared probe: (a) [(d)] Photographs of the extraordinary [ordinary] wave when the 532 nm beam is in the linear regime and (b) [(e)] when it forms a dark spatial soliton. (c) and (f) show the waist of extraordinary and ordinary weak signals versus green excitation, respectively.

it was extraordinarily polarized (co-polarized with the green soliton), it was guided in the channel and propagated in a confined fashion.

3. Conclusions

Using commercially available materials we have shown that azobenzene nematic liquid crystals support efficient nonlinear optical localization based on the induced transformation of *cis* to *trans* isomers in the presence of visible light beams at microwatt power levels. In analogy to "standard" nematic liquid crystals, this nonlinearity is nonlocal and saturable, provides transverse stability and response times well below one second and adjustable with input power. Spatial solitons in azo-LC propagate with moderate attenuation and can be angularly steered and deflected; they undergo long-range attractive interactions with other solitons in the medium, the latter property being incoherent in nature and permitting beam merging independently of the reciprocal phase. Specific mixtures exhibit a self-defocusing nonlinearity and support dark spatial solitons, with waveguiding properties for optical signals outside the absorption band.

"Azo-nematicons" can find interesting applications for auto-aligning fiber couplers, as well as switchable polarizers, optical gates and beam combiners. A detailed model of the photoisomerization-mediated nonlinear response of azo-LC is underway and will be published elsewhere.

Acknowledgments

The authors are grateful to T. J. Bunning (AFOSR) for interest in and support of this study. GA thanks M. Peccianti, A. Alberucci and A. Piccardi.

References

[1] Kivshar, Yu. S., & Agrawal, G. P. (2003). *Optical Solitons*, Academic Press: New York.
[2] Conti, C., & Assanto, G. (2004). In: R. D. Guenther, D. G. Steel, & L. Bayvel (Eds.), *Encyclopedia of Modern Optics*, Vol. 5, Elsevier: Oxford, p. 43.
[3] Boardman, A. D., & Sukhorukov, A. P. (Eds.). (2001). *Soliton Driven Photonics*, Kluwer Academic: Dordrecht.
[4] Stegeman, G. I., Christodoulides, D. N., & Segev, M. (2000). *IEEE J. Sel. Top. Quantum Electron.*, *6*, 1419.
[5] Tabiryan, N. V., Sukhov, A. V., & Zel'dovich, B. Ya. (1986). *Mol. Cryst. & Liq. Cryst.*, *136*, 1.
[6] Khoo, I. C. (1995). *Liquid Crystals: Physical Properties and Nonlinear Optical Phenomena*, Wiley: New York.
[7] Simoni, F. (1997). *Nonlinear Optical Properties of Liquid Crystals*, World Scientific: Singapore.
[8] Peccianti, M., Assanto, G., De Luca, A., Umeton, C., & Khoo, I. C. (2000). *Appl. Phys. Lett.*, *77*, 7.
[9] Assanto, G., & Peccianti, M. (2003). *IEEE J. Quantum Electron.*, *39*, 13.
[10] Assanto, G., Fratalocchi, A., & Peccianti, M. (2007). *Opt. Express*, *15*, 5248.
[11] Assanto, G., & Karpierz, M. (2009). *Liq. Cryst.*, *36*, 1161.
[12] Serak, S. V., & Tabiryan, N. V. (2006). *Proc. SPIE*, *6332*, 63320Y1.
[13] Piccardi, A., Alberucci, A., & Assanto, G. (2010). *Electron. Lett.*, *46*, 790.
[14] Bang, O., Kròlikowski, W., Wyller, J., & Rasmussen, J. J. (2002). *Phys. Rev.*, *E 66*, 046619.
[15] Conti, C., Peccianti, M., & Assanto, G. (2003). *Phys. Rev. Lett.*, *91*, 73901.
[16] Conti, C., Peccianti, M., & Assanto, G. (2004). *Phys. Rev. Lett.*, *92*, 113902.
[17] Peccianti, M., Fratalocchi, A., & Assanto, G. (2004). *Opt. Express*, *12*, 6524.
[18] Peccianti, M., Brzdąkiewicz, K. A., & Assanto, G. (2002). *Opt. Lett.*, *27*, 1460.

[19] Peccianti, M., Conti, C., Assanto, G., De Luca, A., & Umeton, C. (2002). *Appl. Phys. Lett.*, *81*, 3335.
[20] Alberucci, A., Peccianti, M., Assanto, G., Dyadyusha, A., & Kaczmarek, M. (2006). *Phys. Rev. Lett.*, *97*, 153903.
[21] Fratalocchi, A., Piccardi, A., Peccianti, M., & Assanto, G. (2007). *Opt. Lett.*, *32*, 1447.
[22] Fratalocchi, A., Piccardi, A., Peccianti, M., & Assanto, G. (2007). *Phys. Rev.*, *A 75*, 063835.
[23] Pasquazi, A., Alberucci, A., Peccianti, M., & Assanto, G. (2005). *Appl. Phys. Lett.*, *87*, 261104.
[24] Piccardi, A., Alberucci, A., Bortolozzo, U., Residori, S., & Assanto, G. (2010). *Appl. Phys. Lett.*, *96*, 071104.
[25] Piccardi, A., Alberucci, A., Bortolozzo, U., Residori, S., & Assanto, G. (2010). *Photon. Technol. Lett.*, *22*, 694.
[26] Peccianti, M., Dyadyusha, A., Kaczmarek, M., & Assanto, G. (2006). *Nat. Phys.*, *2*, 737.
[27] Peccianti, M., Assanto, G., Dyadyusha, A., & Kaczmarek, M. (2007). *Phys. Rev. Lett.*, *98*, 113902.
[28] Peccianti, M., & Assanto, G. (2007). *Opt. Express*, *15*, 8021.
[29] Piccardi, A., Assanto, G., Lucchetti, L., & Simoni, F. (2008). *Appl. Phys. Lett.*, *93*, 171104.
[30] Hrozhyk, U., Serak, S., & Tabiryan, N. (2006). *Mol. Cryst. Liq. Cryst.*, *454*, 243.
[31] Serak, S. V., Tabiryan, N. V., Peccianti, M., & Assanto, G. (2006). *IEEE Photon. Technol. Lett.*, *18*, 1287.
[32] Landau, L. D., Lifshiz, E. M., & Pitaevskii, L. P. (1984). *Electrodynamics of Continuous*, Pergamon Press: Oxford, UK.
[33] Beeckman, J., Neyts, K., Hutsebaut, X., Cambournac, C., & Haelterman, M. (2005). *IEEE J. Quantum Electron.*, *41*, 735.
[34] Derrien, F., Henninot, J. F., Warenghem, M., & Abbate, G. (2000). *J. Opt. A: Pure Appl.*, *2*, 332.
[35] Tabiryan, N., Hrozhyk, U., & Serak, S. (2004). *Phys. Rev. Lett.*, *93*, 113901.
[36] Peccianti, M., Conti, C., & Assanto, G. (2005). *Opt. Lett.*, *30*, 415.
[37] Peccianti, M., Conti, C., & Assanto, G. (2003). *Opt. Lett.*, *28*, 2231.
[38] Henninot, J. F., Tabiryan, N. V., & Warenghem, M. (1998). *Mol. Cryst. & Liq. Cryst.*, *309*, 189.
[39] Hrozhyk, U., Serak, S., Tabiryan, N., Hoke, L., Steeves, D., & Kimball, B. (2010). *Optics Express*, *18*, 8697.
[40] Hrozhyk, U., Serak, S., Tabiryan, N., Steeves, D., Hoke, L., & Kimball, B. (2009). *Proc. SPIE*, *7414*, 74140L1.
[41] Piccardi, A., Alberucci, A., Tabiryan, N., & Assanto, G. (2011). *Opt. Lett.*, *36*, 1456.